2. EXPERIMENTAL

An x-ray absorption spectrum is measured as the amount of the incoming x-ray which is absorbed by the substrate. The normal set-up to measure x-ray absorption is in transmission mode as sketched in Figure 2.1. The intensity of the x-ray is measured before and after the substrate and the percentage of transmitted x-rays is determined. The x-ray absorption spectrum is generated by repeating the experiment for a series of x-ray energies.

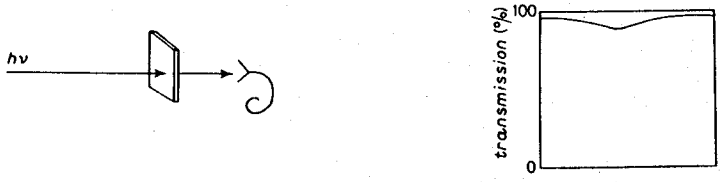

Figure 2.1: Transmission mode experiment of x-ray absorption.

Transmission mode experiments are standard for hard x-rays, though for soft x-rays they are difficult to perform because of the strong interaction of soft x-rays with matter. In order to obtain a detectable signal the substrate has to be thin, typically $\sim 0.1\mu$m. This poses a (too) large technological problem for most materials. Soft x-rays also have a large absorption cross section with air, hence the experiments have to be performed in vaccuum.

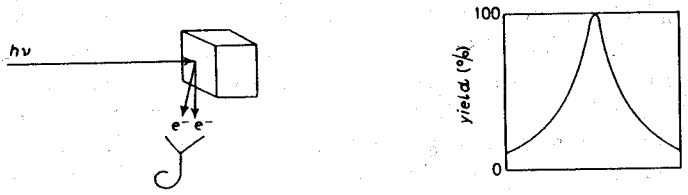

Figure 2.2: Yield-mode experiment of x-ray absorption.

An alternative to the transmission mode experiments has been provided by measuring the decay products of the core hole which is created in the absorption process. The decay of the core hole gives rise to an avalanche of electrons, photons and ions escaping from the

surface of the substrate. Figure 2.2 shows a yield mode experiment of the x-ray absorption cross section, with which it is possible to measure samples of arbitrary thickness.

X-ray absorption experiments have been made since the beginning of this century, but they were severely restricted because the only available intense x-ray sources had only a restricted set of sharply defined energies. The advent of synchrotron radiation sources, which provide an intense and continuum spectrum of electromagnetic radiation, created the possibility of improving immensely the x-ray absorption spectra. Additionally high-resolution monochromators dedicated to synchrotron radiation have been developed. In this chapter the various experimental aspects of the x-ray absorption experiments are discussed. To be discussed are:

- synchrotron radiation
- x-ray monochromators
- sample conditions
- detection techniques

2.1. Synchrotron radiation

Synchrotron radiation is produced when a charged particle, with an energy $E \gg mc^2$, is deflected in a magnetic field. The development of synchrotron radiation is based on the work of Ivanenko and Pomaranchuk [1] and Schwinger [2] in the forties [3, 4]. The original synchrotrons were used for high energy physics and the radiation was considered merely as a side product. The experiments which made use of the radiation were performed in a parasitic fashion. However the interesting results which emerged led to the development of dedicated synchrotron radiation sources in the early seventies and the SRS in Daresbury can be considered as the first dedicated storage ring for synchrotron radiation. The original emphasis was on the optimization of the life-time, the current and the energy of the beam. In the early eighties the emphasis switched to an optimization of the brilliance and also to the development of insertion devices to increase the intensity of high energy photons [4]. Figure 2.3 sketches the development of the available x-ray flux during the last century.

Most experiments for this thesis were performed at the Berliner Elektronen-speicherring Gesellschaft für Synchrotronstrahlung (BESSY) [5], which is an electron storage ring with a circumference of about 62 meters. From each of the twelve bending magnets synchrotron radiation is directed to a number of experimental stations. The energy of the electrons stored in the ring is 754 MeV and to keep the electrons in orbit they are accelerated at one point in the ring to compensate the energy-loss due to emission of radiation in the bending magnets. The position of the electrons is corrected, but nevertheless the stored current slowly decreases because of scattering with remnant gas, imperfect orbit correction, etc. The typical life-time at BESSY is two hours.

The deflection of the electrons in the bending magnets creates electromagnetic radiation with an energy-distribution as sketched in figure 2.4 [1, 2, 6]. The critical energy, E_c, is

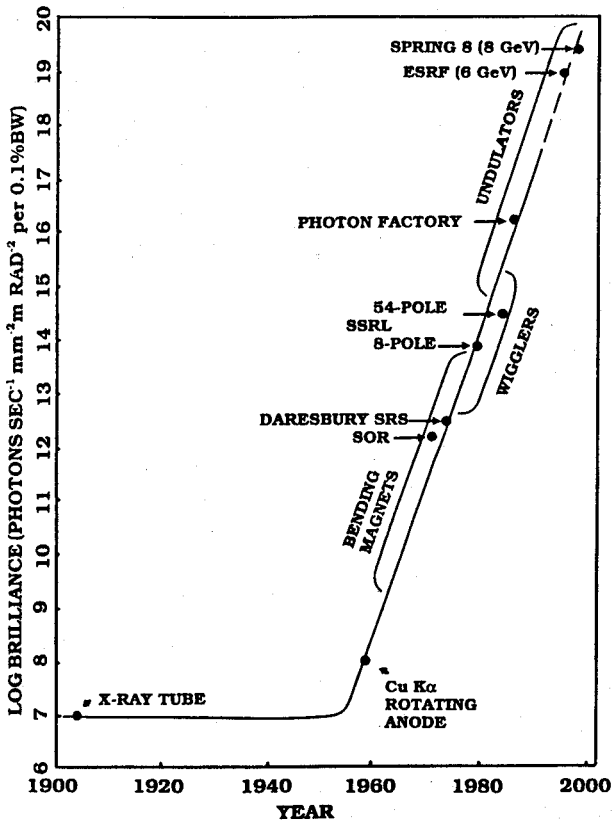

Figure 2.3: The historical development of the brilliance of the available x-ray sources. (Taken from Ref. 4).

determined by the magnetic field in the magnets and the energy of the electrons stored. For BESSY the critical energy is about 600 eV.

Figure 2.5 shows the radial distribution of the radiation for three typical x-ray energies (relative to the critical energy e_c). The radiation in the plane of the orbiting electrons is linearly polarized. Out-of-plane radiation is partly circularly polarized. By selecting part of this out-of-plane radiation, the circularly polarized x-rays can be used. However the intensity of out-of-plane radiation decreases quickly, especially for soft x-rays. The intensity of the circularly polarized x-rays can be increased with the use of special insertion devices such as asymmetric wigglers.

2.2. X-ray monochromators

In order to perform soft x-ray absorption measurements of the oxygen $1s$ edge and the metal $2p$ edges of $3d$-metal oxides, it is crucial that the soft x-rays are monochromatized with high resolution. The edges of interest lie in the difficult energy range in between 200 and 1000 eV, that is in between the traditional regions of grating monochromators ($E < 200$ eV)

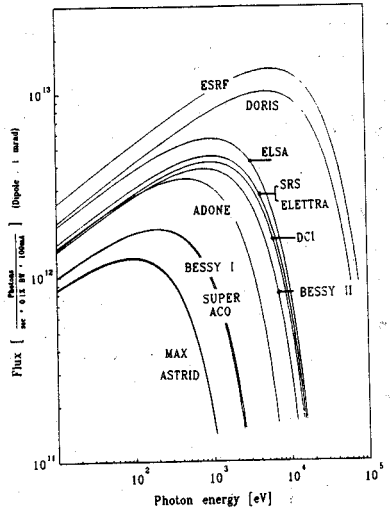

Figure 2.4:
Intensity distribution of the radiation in the European synchrotron radiation facilities. ESRF, ELETTRA and BESSY II are as yet not operational. DORIS and ELSA are used parasitically.
(Taken from Ref. 4).

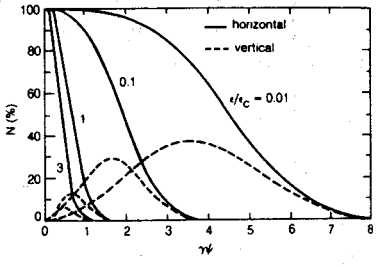

Figure 2.5: Radial distribution of intensity. $\gamma\psi$ is the angle (in mrad) with the plane of the electron-orbit.

and crystal monochromators ($E > 800$ eV).

Crystal monochromators

For energies above 800 eV the usual way to monochromatize the x-ray is by means of a double crystal monochromator. The x-ray beam impinges on the first crystal and the x-ray energy which satisfies Braggs equation ($n\lambda = 2dsin\theta$) is reflected. In principle one crystal is enough to monochromatize the beam; the second crystal improves the resolution by a factor of $1/\sqrt{2}$ but it is used primarily because it allows for a constant direction of the outgoing monochromatized x-ray. The energy range of the double crystal monochromator is defined by the lattice spacing of the crystals used, given that the angle of incidence (θ) is limited between 10 and 80 degrees. For energies above 2 keV artificial silicon crystals ($2d = 6.271$ Å) are used. The difficult energy range in between 800 and 1500 eV is covered by natural beryl crystals ($2d = 15.95$ Å). For energies lower than 800 eV one has to use crystals with a lattice spacing larger than beryl. The organic crystals with this property are

however not resistant to the full power of the synchrotron beam. A solution to this problem has been found by using an artificial multilayer as a pre-monochromator [8]. Although the double crystal monochromators with organic crystals reach a rather good resolution of about $1 : 10^3$, its development has been largely overtaken by recent developments with grating monochromators.

Grating monochromators

The monochromatizing element is in this case an artificial grating with typically 1000 lines per mm ($2d \approx 5 \cdot 10^{-7}$ meter). The soft x-ray range can be covered by using the grating monochromators in grazing incidence ($\theta \rightarrow 0$). The grazing incidence grating monochromators are divided according to the shape of the grating, which can be toroidal, plane or circular. The toroidal grating monochromators (TGM's) dominate in the energy range up to 200 eV. At present the energy region in between 200 eV and 800 eV is best served with either a plane grating monochromator like the SX700, or with a cylindrical (or spherical) grating as is present in the DRAGON.

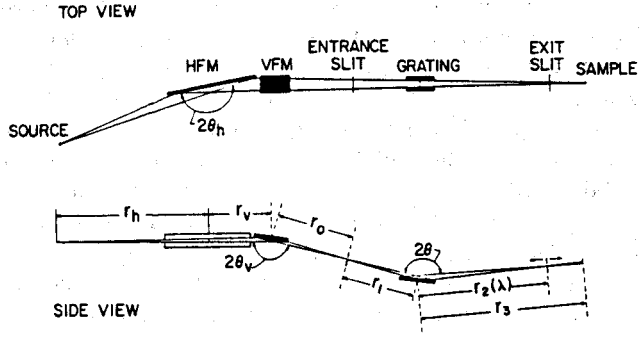

Figure 2.6: Lay-out of the DRAGON monochromator (Taken from Ref. 10).

Part of the experiments have been performed on the DRAGON monochromator [9,10] at the National Synchrotron Light Source (NSLS) at Brookhaven. The DRAGON monochromator reached an unprecedented high resolution of $1 : 10^4$ for the soft x-ray range. It is based on a novel design for a soft x-ray monochromator using cylindrical optical elements. The idea was to design a monochromator with a relatively simple arrangement of optical components [9]. Figure 2.6 sketches the lay-out of the DRAGON. The entrance slit improves the resolution by making the monochromator less dependent on the source size. The exit slit moves during an energy-scan. The mirrors are situated before the grating which facilitates the monochromator positioning to out-of-plane (circularly polarized) radiation. A design in which the beam is split in the mirrorbox and radiation from above and below the

synchrotron plane is guided to the sample simultaneously, that is using a switching device, is under construction [12].

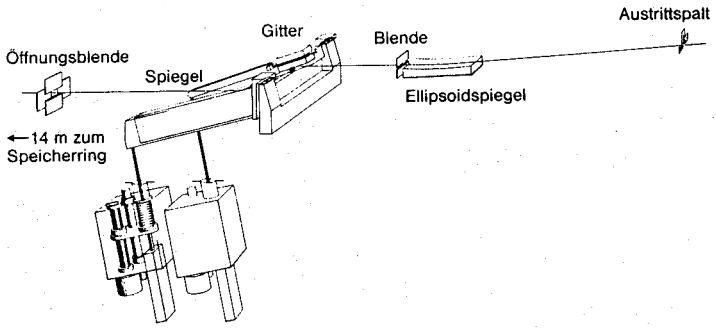

Figure 2.7: Lay-out of the SX700 monochromator. (Taken from Ref. 15).

The experiments at BESSY have been performed with the SX700 monochromators [13, 14], which were designed to monochromatize the synchrotron radiation onto a fixed exit slit, without the necessity of an entrance slit. This can be achieved by a combined movement of the plane grating and the mirrors. Figure 2.7 sketches the lay-out of the SX700. The first plane pre-mirror is used to satisfy the focusing condition of the plane grating [13]. The second elipsoidal mirror refocuses the radiation onto the curved exit slit. The resolution is mainly source limited because there is no entrance slit. The resolution of the SX700(I) is about $1 : 10^3$ and the SX700(II) monochromator has an improved resolution of about $1 : 10^4$. A resolution of $1 : 10^4$ is at present reached by the DRAGON-like monochromators at NSLS-Brookhaven and at SSRL-Stanford [11]. The SX700-based monochromators which obtain a similar resolution can be found at BESSY-Berlin, ISA-Aarhus and MAXLAB-Lund.

2.3. Measurement conditions

All soft x-ray experiments have been performed in ultra high vaccuum, with a typical pressure 10^{-10} torr. It is necessary to work under ultra high vaccuum conditions to assure a clean surface because the detection (total electron yield) is rather surface sensitive. As far as the penetration of the soft x-ray is concerned it is in principle possible to perform experiments in a vacuum of 10^{-5} torr. The measured materials are single crystals or sintered polycrystalline pellets. They are scraped in vaccuum with an alumina or a diamond file. For angular dependent studies on single crystals scraping cannot be used and preferably the sample should be cleaved in situ. If surface cleanliness can not be guaranteed the polarization dependent measurements on the single crystal can be performed and afterwards the sample is scraped and remeasured to check for surface contamination. If not checked for surface cleanliness, total electron yield data from unscraped samples should be treated with

extreme caution. The problems concerning surface cleanliness can be avoided by measuring in fluorescence yield (see next section).

Effects from exposure to the x-ray beam

During an x-ray absorption measurement the dose of soft x-rays which is impinging on the sample is relatively low because the experiments are performed with high resolution and only an extremely small proportion of the beam reaches the sample. Due to the high efficiency of total electron yield this is still enough to measure a spectrum in typically 15 minutes. Beam damage effects can be neglected, given that the sample is not exposed to the white light, which at the present synchrotrons has a radiation dose of typically 10^{17} photons/cm^2. Depending on the material this dose will cause moderate to severe damage [16]. Also charging problems are in general not crucial for x-ray absorption experiments, in contrast to XPS. However the samples should be grounded to prevent macroscopic charging effects.

2.4. Detection techniques

As sketched in figure 2.2 the absorption cross section can be measured by means of electrons which escape from the surface as a result of the decay of the core hole. Instead of electrons, also photons or ions can be detected and the electron, fluorescence and ion yield methods present an alternative to the transmission mode experiments. In this section the different methods are discussed, specifically with regard to the conditions under which a specific yield measurement represents the x-ray absorption cross section. Closely related to this is the probing depth of the specific yield method. That transmission mode experiments are indeed difficult for soft x-ray energies is clear from the analysis of the manganese $2p$ x-ray absorption spectra of MnF_2 as given by Nakai et al. [18]. They used transmission mode detection through a thin film of about 2000 Å. From comparison with theory as well as with yield experiments (see section 5.1), the spectrum given in Ref. 18 is found to be completely saturated.

Auger electron yield

The theoretically clearest yield method is a measurement of the intensity of a specific Auger decay channel of the core hole. The energy of the Auger electron is not dependent on the energy of the incoming x-ray and from the universal curve [18] it is found that the mean free path of a 500 eV Auger electron is of the order of 20 Å. Hence the number of Auger electrons emitted is equal to the number of core holes which are created in the first 20 Å from the surface. Because the mean free path of the incoming x-ray is of the order of 1000 Å, the number of core holes created in the first 20 Å is equal to the absorption cross section. Effectively the Auger electron yield method is a measurement of only 20 Å of material, hence the Auger electron yield is rather surface sensitive.

Fluorescence Yield

Instead of the Auger decay also the fluorescent decay of the core hole can be used as the basis for the absorption measurement. The amount of fluorescent decay is increased with energy [19], and a comparison of the amount of Auger decay with fluorescent decay shows that for the atomic number $Z \leq 20$ Auger decay dominates for all core levels and for $Z \leq 50$ Auger decay dominates all edges apart the K edges for which fluorescent decay starts to dominate [20]. Thus for the $3d$-metals, the K edges show strong fluorescence and all other edges mainly Auger decay. The photon created in the fluorescent decay has a mean free path of the same order of magnitude as the incoming x-ray, which excludes any surface effect. On the other hand it means that there will be large saturation effects if the sample is not dilute. That is, in the limit that there is only absorption process, all x-rays photons which enter the material contribute to the fluorescence yield signal, hence its intensity will not be equal to the absorption cross section. The relation between the intensity of the fluorescence yield (I_f) and the absorption cross section (μ) is [21]:

$$I_f \sim \frac{\mu_x(E)}{\mu_x(E) + \mu_b(E) + \mu_x(E_f) + \mu_b(E_f)} \tag{2.1}$$

For dilute materials, that is if the the background absorption (μ_b) dominates the absorption of the specific edge (μ_x), the measured intensity is approximately equivalent to the absorption coefficient ($I_f \sim \mu_x$). For less dilute materials the spectral shape is modified and the highest peaks will appear compressed with respect to the lower peaks, known as saturation effects. For a given material the background absorption is known and in principle can be corrected for afterwards. However this correction procedure affects the statistics considerably. For concentrated systems, ($\mu_x > \mu_b$), the spectral modifications are too large for a sensible analysis. The $M_{4,5}$ edges of rare earths and to a lesser extend also the the $L_{2,3}$-edges of transition metals are relatively strong, hence the fluorescence yield signal will be completely saturated for the pure metals. Also the binary oxides and other compounds with low-Z elements only will show distorted x-ray absorption spectra. The oxygen K edge of metal oxides will show relatively small saturation effects, especially if some high-Z elements are present as is the case for $YBa_2Cu_3O_{7-\delta}$ and related compounds [22]. Equation 2.1 shows that apart from saturation effects, there can be effects due to so-called self-absorption. If the fluorescent decay of a core hole takes place at an energy (E_f) which is strongly reabsorbed, the spectral shape is modified in a rather complicated manner and the spectrum is difficult to interpret.

Though fluorescent yield is complicated for concentrated materials due to its large escape depth. On the other hand the large escape depth makes fluorescence yield extremely suited for the measurement of impurities, which are difficult to measure with a surface sensitive technique such as Auger yield. The suitability of fluorescence yield for impurities, for example metal ions in bioinorganical cluster compounds or even complete enzymes, has led to the large efforts in the development of fluorescence yield detectors [23].

Ion yield

A third decay product of the core holes are ions. If the absorption process takes place in the bulk and the core hole decays via an Auger process a positively charged ion is formed, but due to further decay and screening processes the original situation will be restored after some time. However if the absorption process takes place at the surface, the possibility exists that the atom which absorbes the x-ray is ionized by Auger decay and escapes from the surface before relaxation processes can bring it back to the ground state. If the escaping ions are analysed as a function of x-ray energy the signal will again be related to the absorption cross section. Because only atoms from the top-layer are measured, ion yield is extremely surface sensitive. The mere possibility of obtaining a measurable signal from ion yield means that the surface is irreversibly distorted, but as there are of the order of 10^{13} surface atoms per mm^2, this does not necessarily mean that a statistically relevant proportion of the surface is modified. From these considerations it is clear that the possibility of ion yield will be highly material dependent. In section 5.4 ion yield is used to study the calcium atoms in the surface layer of CaF_2.

2.4.1. Total electron yield

The most abundant yield detection technique, which is also the most unclear in its nature, is total electron yield. The difference with Auger electron yield is that the energy of the outgoing electrons is not selected and simply all escaping electrons are counted. It is clear that the signal is dominated by secondary electrons which are created in the cascade process of the Auger decay electrons [24, 25]. The ease of detection and the large signal make total electron yield a much used technique, but questions which remain are the specific processes which take place and specifically the probing depth and the related surface sensitivity are only roughly known. A rough estimate for the probing depth is to use the Auger probing depth as the lower boundary and something of the order of 200 Å as the upper boundary. As the creation, migration and escape of secondary electrons will be highly material dependent, the probing depth of total electron yield will certainly be material dependent too.

To study the mean probing depth of total electron yield quantitatively the oxygen K edge of thin layers of Ta_2O_5 on tantalum metal has been studied [26]. The tantalum oxide overlayers can be prepared with great accuracy and they are extremely stable with respect to further oxidation if the layers have a thickness of 20 Å or more [28]. The oxygen K edge of samples with a Ta_2O_5-thickness ranging from 0 to 1200 Å have been measured. To increase the reliability of the data the spectra have been measured several times. Figure 2.8 shows the results for a layer thickness in between 20 and 80 Å. Layer thicknesses of more than 80 Å (160 Å, 320 Å, etc) give identical results to the 80 Å sample. The 10 Å layer has an intensity equal to the 20 Å layer which indicates additional oxidation.

Analysis of the data points reveals that total electron yield is already saturated for layers of the order of 40 Å, which is shorter than often assumed. It is probable that the probing depth of total electron yield is similar for the oxygen K edge of other oxides. It is concluded that the probing depth of total electron yield detection of soft x-ray absorption in oxides is of the order of 40 Å. More details concerning the processes which determine the probing

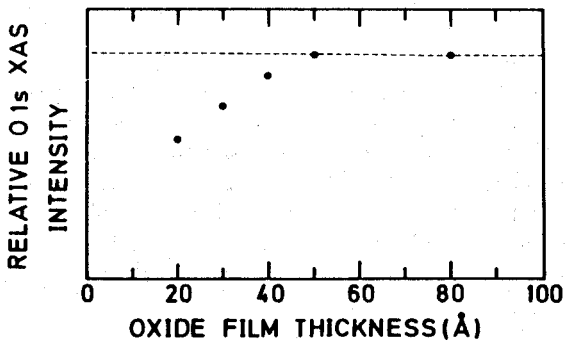

Figure 2.8: Relative oxygen K edge x-ray absorption intensity as a function of the thickness of the Ta_2O_5 layer. (Taken from Ref. 26).

depth are given in Refs. [24–27]. In conclusion table 2.1 gives the best estimates of the probing depths of the different yield methods if applied to $3d$-metal oxides.

Detection technique	Probing depth
Ion yield	~ 2 Å
Auger electron yield	~ 20 Å
Total electron yield	~ 40 Å
Fluorescence yield	> 1000 Å

Table 2.1: Probing depths of yield detection of soft x-ray absorption experiments of $3d$-metal oxides

References

[1] D. Ivanenko and J. Pomeranchuk, *Phys. Rev.* **65**, 343 (1944).
[2] J. Schwinger, *Phys. Rev.* **70**, 798 (1946); *ibid.* **75**, 1912 (1949).
[3] E.E. Koch, B. Kunz and B. Sonntag, *Phys. Reports* **29**, 153 (1977).
[4] I.H. Munro, C.A. Boardman and J.C. Fuggle, *World Compendium of Synchrotron Radiation Facilities*, (European Synchrotron Radiation Society, 1991).
[5] S. Bernstorff et al., *Physica Scripta* **36**, 15 (1987).
[6] I.M. Ternov, V.V. Mikhailov and V.R. Khalilov, *Synchrotron Radiation and its Applications* (Harwood Academic Publishers, 1985).
[7] Jeroen Goedkoop, PhD. thesis *X-ray dichroism of rare earth materials* (University of Nijmegen, 1989).
[8] G. van der Laan, J.B. Goedkoop and A.A. MacDowell, *J. Phys. E.* **20**, 1496, (1987).
[9] C.T. Chen, *Nucl. Instr. Meth. A.* **256**, 595 (1987).
[10] C.T. Chen and F. Sette, *Rev. Sci. Instr.* **60**, 1616 (1989); C.T. Chen and F. Sette, *Physica Scripta* **T31**, 119 (1990).

[11] P.A. Heimann *et al.*, *Physica Scripta* **T31**, 127 (1990).
[12] The so-called double headed DRAGON is under construction; C.T. Chen, F. Sette and N.V. Smith, *Applied Optics* **29**, 4235 (1990).
[13] H. Petersen, *Opt. Commun.* **40**, 402 (1982); German Patent No 30 45 931, European Patent No. 00 53 723, US Patent No. 4,553,253.
[14] H. Petersen, *Nucl. Instrum. Meth. A.* **246**, 260 (1986).
[15] Reimund Torge, Fritz Riemer, Erich Heynacher and Wolfgang Opitz, *Zeiss Inform.* **29**, 55 (1986).
[16] F.J. Himpsel, U.O. Karlsson, A.B. McLean, L.J. Terminello, F.M.F. de Groot, M. Abbate, J.C. Fuggle, J.A. Yarmoff, B.T. Thole and G.A. Sawatzky, *Phys. Rev. B.* **43**, 6899 (1991).
[17] S.-I. Nakai, A. Kawata, M. Ohashi, M. Kitamura, C. Sugiura, T. Mitsuishi and H. Maezawa, *Phys. Rev. B.* **37**, 10895 (1988).
[18] M.P. Seah and W.A. Dench, *Surf. Interface Anal.* **1**, 2 (1979).
[19] P.H. Citrin, P. Eisenberger and B.M. Kincaid, *Phys. Rev. Lett.* **36**, 1346 (1976).
[20] J.C. Fuggle, *Core Level Spectroscopies and Synchrotron Radiation*, in: *Proc. Int. School of Physics*, Ed. R. Rosei (N. Holland, Amsterdam, 1990).
[21] J. Jaklevic, J.A. Kirby, M.P. Klein, A.S. Robertson, G.S. Brown and P. Eisenberger, *Solid State Comm.* **23**, 679 (1977).
[22] L. Tröger, D. Arvanitis, H. Rabus, L. Wenzel and K. Baberschke, *Phys. Rev. B.* **41**, 7297 (1990).
[23] S.P. Cramer, O. Tench and G.N. George, *Nucl. Instr. Meth. A.* **266**, 586 (1988); S.P. Cramer, H. Kraner, S.J. George, L. Rogers, S. Rescia, V. Radeka, M. Yocum, J. Coloresi, O. Tench and O.C. Mullins in: *X-ray Absorption Fine Structure*, Ed. S.S. Hasnain, (Ellis Horwood, Chichester, 1991); page 640.
[24] A. Erbil, G.S. Cargill III, R. Frahm and R.F. Boehme, *Phys. Rev. B.* **37**, 2450 (1988).
[25] B.L. Henke, J. Liesegang and S.D. Smith, *Phys. Rev. B.* **19**, 3004 (1979).
[26] M. Abbate, J.B. Goedkoop, F.M.F. de Groot, M. Grioni, J.C. Fuggle, S. Hoffman, H. Petersen and M. Sacchi, submitted.
[27] A. Krol, C.J. Sher and Y.H. Kao, *Phys. Rev. B.* **42**, 3829 (1990).
[28] J.M. Sanz and S. Hoffman, *Surf. Interface Anal.* **5**, 210 (1983).